

Electrostatic Potential as Solvent Descriptor to Enable Rational Electrolyte Design for Lithium Batteries

Yanzhou Wu, Qiao Hu, Hongmei Liang, Aiping Wang, Hong Xu, Li Wang,*
and Xiangming He*

Artificial intelligence/machine learning (AI/ML) applied to battery research is considered to be a powerful tool for accelerating the research cycle. However, the development of appropriate materials descriptors is often the first hurdle toward implementing meaningful and accurate AI/ML. Currently, rational solvent selection remains a significant challenge in electrolyte development and is still based on experiments. The dielectric constant (ϵ) and donor number (DN) in electrolyte design are insufficient. Finding theoretically computable solvent descriptors for evaluating Li^+ solvation is a significant step toward accelerating electrolyte development. Here, based on the electrostatic interaction between Li^+ and solvent, the electrostatic potential (ESP) of electrolyte solvent is calculated by density functional theory calculations and reveals significant regularity. ESP as a direct and simple solvent descriptor for conveniently designing electrolytes is proposed. The lowest negative electrostatic potential (ESP_{\min}) ensures the nucleophilic capacity of the solvating solvent and the weak ESP_{\min} means decreased solvation energy. Weak ESP_{\min} and strong highest positive electrostatic potential (ESP_{\max}) are the main characteristics of non-solvating antisolvents. Using the plot of $\text{ESP}_{\min} - \text{ESP}_{\max}$ strong solvating solvent, weakly solvating solvent, or antisolvent are identified that have been used in electrolyte engineering. This solvent descriptor can boost AI/ML to develop high performance electrolytes.

1. Introduction

Substantial progress has been made in the use of lithium-ion batteries (LIBs) as electrochemical energy storage devices.^[1–4] New electrode materials such as lithium transition metal oxide cathodes (LiCoO_2 , LiMnO_2 , $\text{LiNi}_x\text{Co}_y\text{Mn}_{1-x-y}\text{O}_2$), sulfur cathodes,^[5–7] silicon anodes,^[8,9] and lithium metal anodes^[10–12] have been investigated in the pursuit of higher energy density or more stringent application conditions. However, the implementation of a new battery system is always hindered by undesired electrode/electrolyte interfacial reactions. Thus, there

is an urgent need to optimize electrolytes to match evolving battery systems.^[10,13–16] Electrolyte engineering is one of the hotspots in the field of battery research, including various additives,^[17–20] new fluorinated solvents,^[21–26] new lithium salts,^[27,28] etc. Importantly, the strategy of anion-derived interfacial chemistry refreshed the electrolyte framework and lead to significant progress in both traditional LIBs and new battery chemistry. By introducing anions into the Li^+ solvation structure, such as high-concentration electrolytes (HCEs),^[29,30] localized high-concentration electrolytes (LHCEs),^[31–33] and weakly solvating electrolytes (WSEs),^[34,35] organic-rich solid electrolyte interphase (SEI)/ cathode-electrolyte interphase (CEI) can be rationally regulated. There are a limited number of suitable anions, solvents play an essential role in determining anion-derived interfacial chemistry. To date, the design and selection of electrolytes have mainly been based on experiments. This conventional trial-and-error process of electrolyte design can make for a long and complex research cycle. The artificial

intelligence/machine learning (AI/ML) methods applied to battery research are considered to be a powerful tool for accelerating the research cycle.^[36,37] To develop appropriate materials descriptors is often the first difficulty toward implementing meaningful and accurate AI/ML methods/models. The general solvent descriptors will help accelerate the development of advanced electrolyte, which is currently still a challenge.

The basic composition of electrolytes for lithium-based batteries includes organic solvents and lithium salts with large anions. The ideal solvents should overcome the electronic interaction between cations and anions to dissolve the salts. Polarity is an important factor in the prediction of the dissolving capability of a solvent, and it describes the inhomogeneity of the charge distribution in solvent molecules. Actually, the concept of polarity is very vague and difficult to define. Based on the understanding of solvent chemistry, the dielectric constant (the relative permittivity, ϵ) and donor number (DN) are commonly used instead of polarity to evaluate the dissolving capacity of solvents to solubilize lithium salts (Figure 1).^[38]

Y. Wu, Q. Hu, H. Liang, A. Wang, H. Xu, L. Wang, X. He
Institute of Nuclear and New Energy Technology
Tsinghua University
Beijing 100084, China
E-mail: wang-l@tsinghua.edu.cn; hexm@tsinghua.edu.cn

The ORCID identification number(s) for the author(s) of this article can be found under <https://doi.org/10.1002/aenm.202300259>

DOI: 10.1002/aenm.202300259

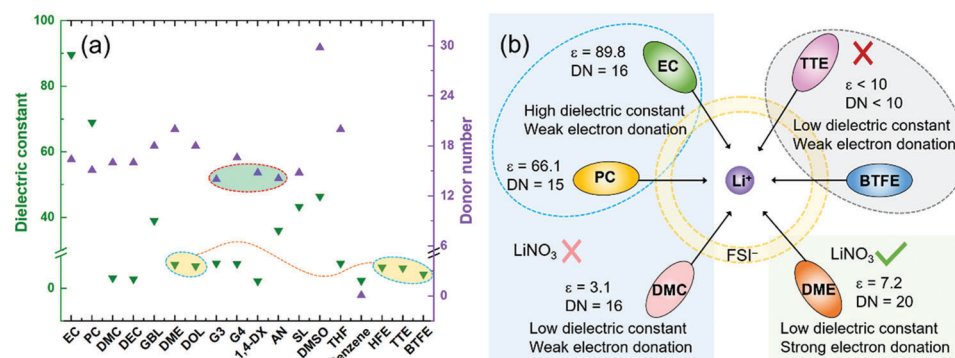


Figure 1. a) Dielectric constant and donor number of some solvents for lithium-ion or lithium-metal batteries. b) Schematic illustration of the relationship among the dielectric properties, electron donation, and salt-dissolving capability of several typical solvents, the discussion above is in the context of LiFSI as the main salt.

Before discussing the ϵ and DN of solvents, the expanded forms of all mentioned acronyms can be checked in Supporting information (Table S2). The ϵ describes a solvent's ability to separate the salt into ions.^[39,40] In conventional electrolytes, solvents are usually polar with moderate ϵ , such as ethylene carbonate (EC), propylene carbonate (PC), acetonitrile (AN), sulfolane (SL), 1,2-dimethoxyethane (DME), dimethyl carbonate (DMC), and ethyl acetate (EA). DN^[41,42] describes the Lewis-type donor properties of a solvent. For example, lithium nitrate (LiNO_3) has a high solubility in ether-based solvents but low solubility in most ester-based electrolytes (Figure 1b). The root cause of this phenomenon is that the ether-based solvents have DN values comparable to that of NO_3^- (21.1 kcal mol⁻¹), such as DME (20.0 kcal mol⁻¹). However, the ϵ or DN is inadequate to describe the dissolution behavior of a specific solvent. For LHCEs, non-solvating hydrofluoroethers (HFEs) have low similar to that of DME, but they have no solubility toward lithium salts. In addition, the DN of 1,4-dioxane (1,4-DX) (14.8 kcal mol⁻¹) is higher than that of AN (14.1 kcal mol⁻¹) (Figure 1a), while lithium bis(fluorosulfonyl)imide (LiFSI) has low solubility in 1,4-DX and forms contact ion pairs even at low concentrations.^[34] Therefore, a physicochemical parameter to comprehensively reflect the dissolving capacity of a solvent is greatly needed to guide electrolyte engineering. Nevertheless, the anion and solvent both act as ligands to construct solvation structure, so solvent coordinates with Li^+ will be significantly affected by different anions. Due to the complexity of different anion interaction model, we expect to simplify the model and carry out a comprehensive discussion in this paper. Thus, LiFSI is selected as the main salt of the electrolyte. In this model, Li^+ -solvents- FSI^- , whether FSI^- participates in solvation structure or not is irrelevant to compare the competitive coordination between different solvents.

To date, some efforts have been made toward identifying design strategies for non-solvating antisolvents by formulating descriptors. Moon et al. employed the normalized molar electronic transition energy (EN T) and Kamlet-Taft Lewis basicity (β)^[43] as critical parameters for choosing optimal non-solvating antisolvents for LHCEs.^[43] Ding et al. reported a descriptor based on the relationship between the relative binding energy and the dielectric constant to qualitatively predict antisolvents.^[44] Although these strategies are helpful for the selection of antisolvents, they cannot be used to describe the action of solvating solvents. An

electrostatic potential (ESP)^[45–47] is induced in the space surrounding a molecule by its nuclei and electrons and reflects an unbalanced distribution of charge. Murray et al. proposed that the most positive surface potential (ESP_{max}) and the most negative potential (ESP_{min}) could be used to measure the polarity of a molecule.^[48] Moreover, the ESP can effectively explain the interaction between Li^+ and solvents in electrolytes.^[49,50] In this work, we utilize density functional theory (DFT) to investigate the ESP of a large number of solvents. The purpose is to provide a simple method to screen the solvent used for electrolytes and afford a clear image of electrolyte engineering. In detail, solvent molecules are qualitatively analyzed in terms of ESP_{max} and ESP_{min} . The results of this work suggest that a diagram of ESP_{min} and ESP_{max} can be used to reliably estimate solvents in electrolytes. The proposed solvent descriptors are expected to be an efficient tool to implement effective and accurate AI/ML models, which accelerate the development of advanced electrolyte for high performance lithium batteries.

2. Results and Discussion

In electrolytes, when a solvent molecule can act as an electron donor to coordinate with Li^+ , the donor unit in question is characterized by a strongly negative surface electrostatic potential. Figure 2 shows the ESP maps of solvating solvents and anti-solvents, including ester-based EC, DMC, EA, and ethyl fluoroacetate (FEA), ether-based DME and 1,4-DX, cyanophoric AN, HFEs as 1,1,2,2-tetrafluoroethyl-2,2,2-trifluoroethyl ether (HFE), 1,1,2,2-tetrafluoroethyl 2,2,3,3-tetrafluoropropyl ether (TTE) and bis(2,2,2trifluoroethyl) ether (BTFE), dichloromethane (DCM) etc. The negative charge of the solvating solvent is mainly localized at the oxygen and nitrogen atoms, and results in a much more negative ESP than that of the antisolvent. For the solvating solvent, the absolute value of the lowest electrostatic potential ($|\text{ESP}_{\text{min}}|$) is much higher than ESP_{max} , ($|\text{ESP}_{\text{min}}| > \text{ESP}_{\text{max}}$). In contrast, the ESP of the antisolvent apparently shows opposite trends, with $|\text{ESP}_{\text{min}}| < \text{ESP}_{\text{max}}$, as the presence of fluorine atoms causes dispersion of the surface negative charge of the oxygen atom so that the negative charge is almost equally dispersed across the oxygen and fluorine atoms. This means that the antisolvent is an unsatisfactory electron donor, consistent with the non-solvating phenomenon mentioned in previous

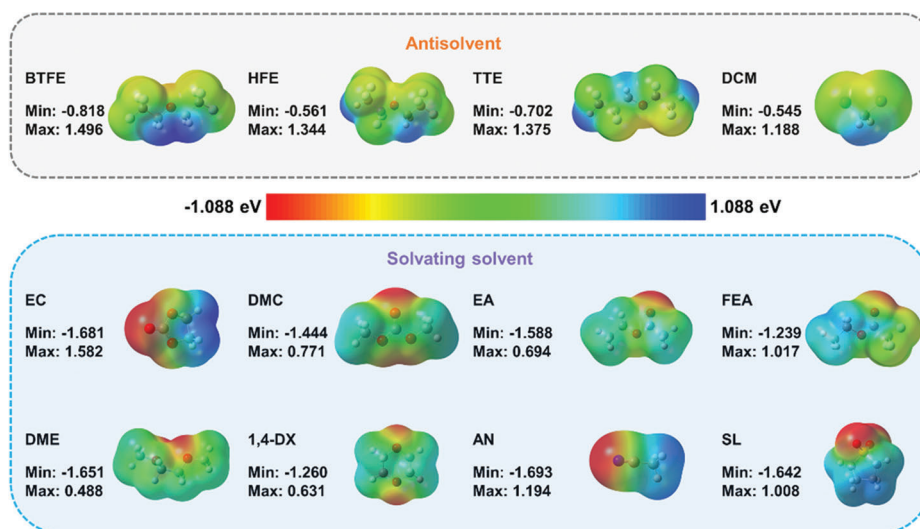


Figure 2. Calculated electrostatic potential maps of organic solvents under vacuum conditions.

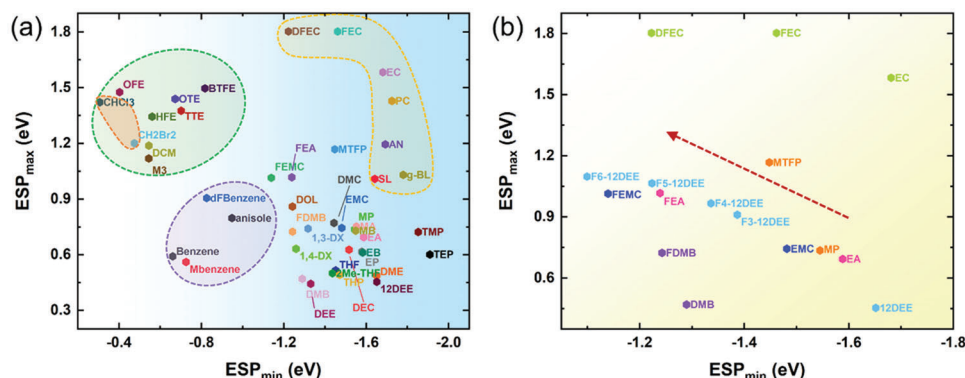


Figure 3. a) Density functional theory-calculated electrostatic potential (ESP) of various solvents under vacuum conditions. b) ESP of fluorinated solvents.

publications.^[33] Therefore, we suppose it is feasible to guide the design of functional electrolytes based on the ESP characteristics of molecules.

To validate the universality of the ESP rule, statistical analyses of numerous solvent molecules are performed using ESP_{min} and ESP_{max} , the full name of solvents and corresponding abbreviations are listed in Table S2 (Supporting Information). As shown in Figure 3a, the distribution of the solvents is quite regular, and the typical solvents are shaded with color. HFEs, as representative antisolvents, such as HFE, TTE and BTFE^[51–54] have been verified to inhibit lithium dendrites and enable a high cycling stability of lithium-metal batteries. In addition, DCM^[55] as a antisolvent successfully enables metal lithium battery (MLB) charging at $-70\text{ }^{\circ}\text{C}$ with high energy-density. These antisolvents are all located in the upper-left corner (green shaded), their ESP_{min} values are less negative and $|ESP_{min}| < ESP_{max}$. Moreover, benzene and 1,2-difluorobenzene (dFBn) have lower affinity to Li^+ and have been demonstrated to be new antisolvents for diluting high-concentrated electrolytes.^[44–56] Anisole has been studied as an additive to protect against overcharging in LIBs, but lithium salts also have low solubility in them. It can be seen that aro-

matic solvents (purple shaded) are characterized by low $|ESP_{min}|$ and ESP_{max} . Thus, these results demonstrate that solvents with weakly negative ESP_{min} are not excellent electron donors and hinder the dissolution of lithium salt, making them suitable antisolvent as expected.

In nonaqueous electrolytes for LIBs, the anions are hardly solvated. The competitive behavior of the solvent and anion solvation determines the solvation structure of Li^+ ions. In conventional 1 M LiPF_6 -carbonate based electrolytes, the dominant solvation structure is that only solvents are involved in the Li^+ solvation sheath and form solvent-separated ion pairs (SSIPs). However, for the WSEs, contact ion pairs (CIPs) and aggregated ion pairs (AIPs) can form even at low concentrations. As shown in Figure 3a, the conventional solvents are mainly distributed on the right side of the diagram with a strongly negative surface electrostatic potential. Note that the positive and negative surface electrostatic potentials of strong polar solvents (yellow shaded) such as EC, PC, and AN are both relatively strong ($|ESP_{min}| \approx ESP_{max}$). For weakly solvating solvents such as diethyl ether (DEE), 1,2-diethoxyethane (12DEE), 1,3-dioxolane (DOL), and 1,4-DX, a significantly decreased ESP_{max} was observed ($|ESP_{min}| \gg ESP_{max}$).

Although using ESP_{min} and ESP_{max} to measure polarity is inaccurate, it is still a useful reference. Generally, dielectric constant is another indicator estimating the polarity of molecule ignoring its limitation. Thus, we further analyze the relationship between ESP_{max} and the dielectric constant, as shown in Figure S4 (Supporting Information), and a positive correlation between them is observed. This result suggests that for weakly polar solvent, the change of the ESP_{max} represent the change of polarity. More specifically, if ESP_{min} is similar, a higher ESP_{max} indicates a greater degree of charge separation, which leads to greater polarity. Such an observation is reasonable to explain the Li^+ solvation sheath structure. A strongly negative ESP_{min} enables a solvent to coordinate with Li^+ , while a change in ESP_{max} indicates a fluctuation in the molecular polarity. For weakly solvating solvents, a low ESP_{max} means low polarity, and anions prefer to connect with Li^+ and form CIPs or AIPs at low concentrations.

The ESP of EC, EA, methyl propionate (MP), 12DEE, and their fluorinated derivatives are presented in Figure 3b. Notably, the ESP_{min} of the fluorinated solvent becomes less negative than that of its analog without substitution, suggesting that fluorine atoms weaken the affinity of solvents coordinating to Li^+ and facilitate Li^+ desolvation. This result is consistent with the recent popular design strategy of solvation regulation.^[57,58] Moreover, the ESP of solvent molecules under both acetone and solution conditions are also evaluated (Supporting information, Figures S1–S3, Supporting Information), and we can see that they show similar trends under vacuum conditions. Consequently, we can roughly distinguish antisolvents, strongly solvating solvents, and weakly solvating solvents by means of a $ESP_{min} - ESP_{max}$ diagram. In addition, we calculate the ESP of several solvent molecules that have never been applied as solvents for LIB electrolytes, such as trichloromethane ($CHCl_3$), dibromomethane (CH_2Br_2), and methylbenzene (Mbenzene), which show charge distribution characteristics similar to those of DCM or benzene and might be considered antisolvent candidates in the future.

Binding energy is a common indicator to evaluate the ability of solvents or anions to be involved in the Li^+ solvation sheath.^[34,59] To further evaluate the rationality of using ESP as a solvent indicator, we discuss the relationship between the binding energy and ESP. Here, the optimized chemical structures of typical Li^+ -solvent complexes are shown in Figure 4a. Under vacuum conditions, the solvation effect is ignored, and ϵ is considered to be fixed. The results show that Li^+ prefers to interact with C=O, C=O, P=O, and C≡N groups. As shown in Figure S5 (Supporting Information), the Li^+ -solvent conformations under acetone conditions are similar to the above results. Such a tendency agrees with the distribution of negative charges on the surface of solvating solvents (Figure 2). Figure 4b shows the corresponding binding energy of the above-optimized Li^+ -solvent complexes in a vacuum. A low binding energy means a weak interaction between Li^+ and solvents, which favors the coordination of anions in the Li^+ solvation sheath. As depicted in Figure S6 (Supporting Information), a nearly linear relationship, with a slope of 1.2, is obtained in the binding energy – ESP_{min} plot. This indicates that it is reasonable to use ESP_{min} to assess the interaction between the solvent and Li^+ .

Moreover, Figure 5 illustrates our general idea for choosing the ESP as a descriptor. For lithium battery electrolytes, solvent molecules interacting with ions are generated mainly through

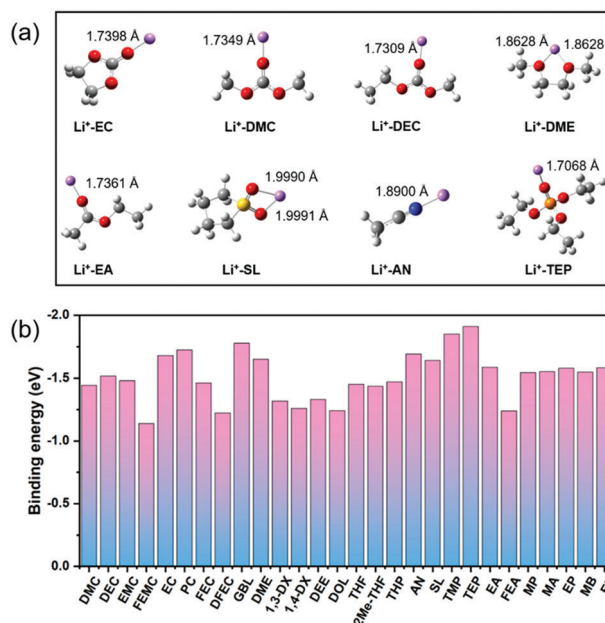


Figure 4. a) Optimized chemical structures of various Li^+ -solvent complexes under vacuum conditions. Li, O, H, S, N, and P atoms are shown in purple, red, gray, yellow, blue, and orange, respectively. b) Binding energies of Li^+ -solvent complexes calculated by DFT in a vacuum.

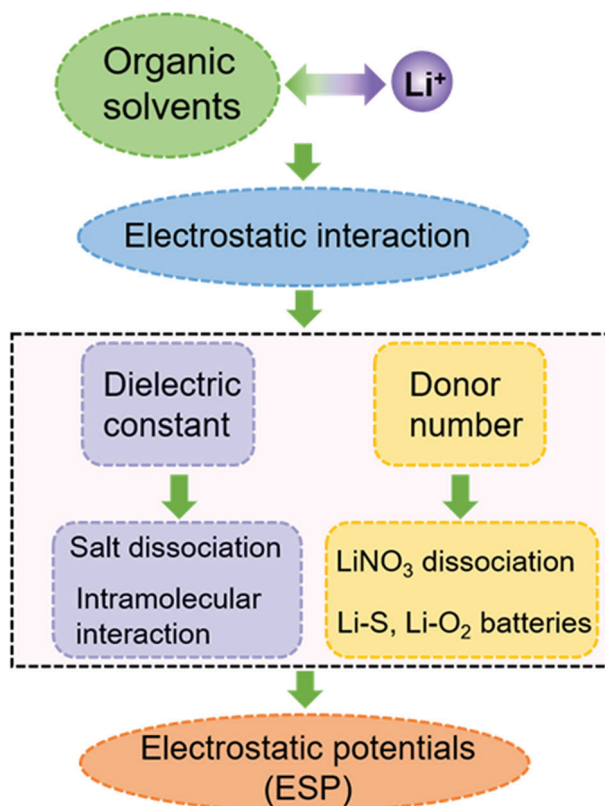


Figure 5. The general guidelines for choosing ESP as a descriptor.

electrostatic interactions. Both the ϵ and the DN provide information about electrostatic interactions between the donor and acceptor, but each has its own emphasis.^[38–59] ϵ focuses on describing the charge polarization of a molecule in an electric field, while DN reflects the ability of enriched electrons in the solvate to attract Li^+ . Therefore, it is sometimes contradictory to use a single method to evaluate the interaction with the electrolyte. EPS describes the specific location and density of charge on the surface of a molecule. It can be used to characterize the microscopic interaction between the solvate and Li^+ , so it is an essential physico-chemical parameter to evaluate the interactions between components in electrolytes. Based on the above results, we conclude that the electrostatic potential provides an ideal perspective to guide the design of electrolyte solvation structures.

3. Conclusion

In summary, the surface ESP of solvents in electrolyte engineering is investigated using DFT calculations, elucidating the surface charge characteristics of solvating solvents. The generated solvent diagram shows obvious distribution regularities. As revealed by the calculation results, the surface charge distribution of antisolvents is characterized by $|\text{ESP}_{\min}| \ll \text{ESP}_{\max}$. We apply this law to predict several novel antisolvent molecules that may become the next generation of antisolvent candidates. Furthermore, the change in surface ESP can be used to compare the strength of solvent participation in solvation. A solvating solvent plays the role of electron donor and coordinates with Li^+ and a decrease in ESP_{\min} indicates a low solvation energy. A diagram of binding energy and ESP_{\min} can be used to reliably estimate competitive coordination between solvents in electrolytes. This insight enables us to screen antisolvents, strongly solvating solvents, and weakly solvating solvents. Therefore, analysis of the ESP of solvents is a simple method for screening solvents and regulating the solvation structure. Moreover, a stable solvation structure is the result of competitive coordination between anions and solvents. The discussion of anion reinforced solvation for electrolytes is beyond the scope of this work. To further increase the understanding of the ESP model, we have introduced a discussion of anions in another work, which will not be discussed here.

4. Experimental Section

Density functional theory (DFT) calculations were performed using the Gaussian16 program.^[60] The geometrical structures and the binding energy were optimized and calculated at the B3LYP/6-311++G (d, p) level of theory.^[61,62] To improve the accuracy of the electrostatic potential (ESP), the stable conformations obtained above were used as the initial structure for single-point calculations at the B3LYP/def2tzvp level. Simultaneously, the implicit solvation model (SMD) was used to describe the solvation effect, and the parameters for SMD are listed in Table S1 (Supporting Information). Based on the above results, the ESP of the solvent was analyzed by using Multiwfn software.^[63] In addition, the binding energy (E_b) was attributed to electrostatic interactions (ion–dipole interaction) between the solvent and Li^+ in electrolytes and was defined as follows:

$$E_b = E_{x-y} - E_x - E_y \quad (1)$$

where E_{x-y} is the total energy of the Li^+ -solvent complexes and E_x and E_y are the energies of components x and y, respectively.

Supporting Information

Supporting Information is available from the Wiley Online Library or from the author.

Acknowledgements

The authors would like to express gratitude to the National Natural Science Foundation of China (Nos. 22279070 (L.W.), U21A20170(X.H.) and 52073161(H.X.)), the Ministry of Science and Technology of China (No. 2019YFA0705703(L.W.)), and the Postdoctoral Research Foundation of China (No. 2022M720080(A.W.)). The authors would also like to thank the “Explorer 100” cluster system of Tsinghua National Laboratory for Information Science and Technology for facility support.

Conflict of Interest

The authors declare no conflict of interest.

Author Contributions

L.W. and X.H. conceived the idea of this research, and edited and reviewed the manuscript. Y.W. carried out the DFT calculations, analyzed the data, and drafted this manuscript. Q.H., H.L., and A.W. offered experiential electrolyte formulations. All authors discussed the results.

Data Availability Statement

The data that support the findings of this study are available in the supplementary material of this article.

Keywords

density function theory, electrolytes, electrostatic potential, lithium batteries, solvent descriptors

Received: January 25, 2023
Revised: March 25, 2023
Published online: April 14, 2023

- [1] A. Manthiram, X. Yu, S. Wang, *Nat. Rev. Mater.* **2017**, 2, 16103.
- [2] M. Winter, B. Barnett, K. Xu, *Chem. Rev.* **2018**, 118, 11433.
- [3] M. Hu, X. Pang, Z. Zhou, *J. Power Sources* **2013**, 237, 229.
- [4] X. Fan, C. Wang, *Chem. Soc. Rev.* **2021**, 50, 10486.
- [5] H. Yamin, A. Gorenshtein, J. Penciner, Y. Sternberg, E. Peled, *J. Electrochem. Soc.* **1988**, 135, 1045.
- [6] M. Cuisinier, P. E. Cabelguen, B. D. Adams, A. Garsuch, M. Balasubramanian, L. F. Nazar, *Energy Environ. Sci.* **2014**, 7, 2697.
- [7] S.-E. Cheon, K.-S. Ko, J.-H. Cho, S.-W. Kim, E.-Y. Chin, H.-T. Kim, *J. Electrochem. Soc.* **2003**, 150, A796.
- [8] M. N. Obrovac, L. Christensen, *Electrochem. Solid-State Lett.* **2004**, 7, A93.
- [9] X. Li, M. Gu, S. Hu, R. Kennard, P. Yan, X. Chen, C. Wang, M. J. Sailor, J. G. Zhang, J. Liu, *Nat. Commun.* **2014**, 5, 4105.

- [10] X. B. Cheng, R. Zhang, C. Z. Zhao, Q. Zhang, *Chem. Rev.* **2017**, 117, 10403.
- [11] W. Xu, J. Wang, F. Ding, X. Chen, E. Nasybulin, Y. Zhang, J.-G. Zhang, *Energy Environ. Sci.* **2014**, 7, 513.
- [12] Y. Jie, X. Liu, Z. Lei, S. Wang, Y. Chen, F. Huang, R. Cao, G. Zhang, S. Jiao, *Angew. Chem., Int. Ed.* **2020**, 59, 3505.
- [13] X. Zhang, L. Zou, Y. Xu, X. Cao, M. H. Engelhard, B. E. Matthews, L. Zhong, H. Wu, H. Jia, X. Ren, P. Gao, Z. Chen, Y. Qin, C. Kompella, B. W. Arey, J. Li, D. Wang, C. Wang, J. G. Zhang, W. Xu, *Adv. Energy Mater.* **2020**, 10, 2000368.
- [14] T. Hou, G. Yang, N. N. Rajput, J. Self, S.-W. Park, J. Nanda, K. A. Persson, *Nano Energy* **2019**, 64, 103881.
- [15] K. Xu, *Chem. Rev.* **2014**, 114, 11503.
- [16] L. Wang, X. He, *Curr. Opin. Electrochem.* **2021**, 30, 100783.
- [17] N. Piao, S. Liu, B. Zhang, X. Ji, X. Fan, L. Wang, P.-F. Wang, T. Jin, S.-C. Liou, H. Yang, J. Jiang, K. Xu, M. A. Schroeder, X. He, C. Wang, *ACS Energy Lett.* **2021**, 6, 1839.
- [18] G. Xu, X. Wang, J. Li, X. Shangguan, S. Huang, D. Lu, B. Chen, J. Ma, S. Dong, X. Zhou, Q. Kong, G. Cui, *Chem. Mater.* **2018**, 30, 8291.
- [19] F. Aupperle, N. von Aspern, D. Berghus, F. Weber, G. G. Eshetu, M. Winter, E. Figgemeier, *ACS Appl. Energy Mater.* **2019**, 2, 6513.
- [20] K. Kim, H. Ma, S. Park, N.-S. Choi, *ACS Energy Lett.* **2020**, 5, 1537.
- [21] P. Xiao, Y. Zhao, Z. Piao, B. Li, G. Zhou, H.-M. Cheng, *Energy Environ. Sci.* **2022**, 15, 2435.
- [22] Z. Yu, W. Yu, Y. Chen, L. Mondonico, X. Xiao, Y. Zheng, F. Liu, S. T. Hung, Y. Cui, Z. Bao, *J. Electrochem. Soc.* **2022**, 169, 040555.
- [23] Y. Zhao, T. Zhou, T. Ashirov, M. E. Kazzi, C. Cancellieri, L. P. H. Jeurgens, J. W. Choi, A. Coskun, *Nat. Commun.* **2022**, 13, 2575.
- [24] N. Piao, X. Ji, H. Xu, X. Fan, L. Chen, S. Liu, M. N. Garaga, S. C. Greenbaum, L. Wang, C. Wang, X. He, *Adv. Energy Mater.* **2020**, 10, 1903568.
- [25] Y. Wu, A. Wang, Q. Hu, H. Liang, H. Xu, L. Wang, X. He, *ACS Cent. Sci.* **2022**, 8, 1290.
- [26] G. Ma, L. Wang, X. He, J. Zhang, H. Chen, W. Xu, Y. Ding, *ACS Appl. Energy Mater.* **2018**, 1, 5446.
- [27] C. Yan, Y. X. Yao, X. Chen, X. B. Cheng, X. Q. Zhang, J. Q. Huang, Q. Zhang, *Angew. Chem., Int. Ed.* **2018**, 57, 14055.
- [28] W. Deng, W. Dai, X. Zhou, Q. Han, W. Fang, N. Dong, B. He, Z. Liu, *ACS Energy Lett.* **2020**, 6, 115.
- [29] J. Wang, Y. Yamada, K. Sodeyama, C. H. Chiang, Y. Tateyama, A. Yamada, *Nat. Commun.* **2016**, 7, 12032.
- [30] Y. Yamada, K. Furukawa, K. Sodeyama, K. Kikuchi, M. Yaegashi, Y. Tateyama, A. Yamada, *J. Am. Chem. Soc.* **2014**, 136, 5039.
- [31] G. Ma, L. Wang, X. He, J. Zhang, H. Chen, W. Xu, Y. Ding, *ACS Appl. Energy Mater.* **2018**, 1, 5446.
- [32] L. Yu, S. Chen, H. Lee, L. Zhang, M. H. Engelhard, Q. Li, S. Jiao, J. Liu, W. Xu, J.-G. Zhang, *ACS Energy Lett.* **2018**, 3, 2059.
- [33] X. Cao, H. Jia, W. Xu, J.-G. Zhang, *J. Electrochem. Soc.* **2021**, 168, 010522.
- [34] Y.-X. Yao, X. Chen, C. Yan, X.-Q. Zhang, W.-L. Cai, J.-Q. Huang, Q. Zhang, *Angew. Chem., Int. Ed.* **2021**, 60, 4090.
- [35] T. D. Pham, A. Bin Faheem, J. Kim, H. M. Oh, K. K. Lee, *Small* **2022**, 18, 2107492.
- [36] T. Lombardo, M. Duquesnoy, H. El-Bouysidi, F. Aren, A. Gallo-Bueno, P. B. Jorgensen, A. Bhowmik, A. Demortiere, E. Ayerbe, F. Alcaide, M. Reynaud, J. Carrasco, A. Grimaud, C. Zhang, T. Vegge, P. Johansson, A. A. Franco, *Chem. Rev.* **2022**, 122, 10899.
- [37] N. Yao, X. Chen, Z. H. Fu, A. Zhang, *Chem. Rev.* **2022**, 122, 10970.
- [38] C. Reichardt, *Solvents and Solvent Effects in Organic Chemistry*, 3rd Edition, Wiley-VCH Verlag GmbH & Co.: KGaA, Weinheim, **2002**.
- [39] A. Jouyban, V. Jouyban-Gharamaleki, M. Khoubnasabjafari, S. Soltanpour, W. E. Acree, *Phys. Chem. Liq.* **2022**, 60, 910.
- [40] A. Jouyban, S. Soltanpour, H. K. Chan, *Int. J. Pharm.* **2004**, 269, 353.
- [41] V. Gutmann, *Coord. Chem. Rev.* **1976**, 18, 225.
- [42] V. Gutmann, *Electrochim. Acta* **1976**, 21, 661.
- [43] J. Moon, D. O. Kim, L. Bekaert, M. Song, J. Chung, D. Lee, A. Hubin, J. Lim, *Nat. Commun.* **2022**, 13, 4538.
- [44] J. F. Ding, R. Xu, N. Yao, X. Chen, Y. Xiao, Y. X. Yao, C. Yan, J. Xie, J. Q. Huang, *Angew. Chem., Int. Ed.* **2021**, 60, 11442.
- [45] J. S. Murray, P. Politzer, *WIREs Comput. Mol. Sci.* **2011**, 1, 153.
- [46] P. Politzer, J. S. Murray, *Theor. Chem. Acc.* **2002**, 108, 134.
- [47] J. S. Murray, P. Politzer, *WIREs Comput. Mol. Sci.* **2017**, 7, e1326.
- [48] J. S. Murray, T. Brinck, P. Lane, K. Paulsen, P. Politzer, *J. Mol. Struct.* **1994**, 307, 55.
- [49] Z. Yu, H. S. Wang, X. Kong, W. Huang, Y. C. Tsao, D. G. Mackanic, K. C. Wang, X. C. Wang, W. X. Huang, S. Choudhury, Y. Zheng, C. V. Amanchukwu, S. T. Hung, Y. T. Ma, E. G. Lomeli, J. Qin, Y. Cui, Z. N. Bao, *Nat. Energy* **2020**, 5, 526.
- [50] C. S. Rustonji, Y. Yang, T. K. Kim, J. Mac, Y. J. Kim, E. Caldwell, H. Chung, Y. S. Meng, *Science* **2017**, 356, 1351.
- [51] X. Cao, P. Gao, X. Ren, L. Zou, M. H. Engelhard, B. E. Matthews, J. Hu, C. Niu, D. Liu, B. W. Arey, C. Wang, J. Xiao, J. Liu, W. Xu, J. G. Zhang, *Proc. Natl. Acad. Sci. U.S.A.* **2021**, 118, e2020357118.
- [52] X. Ren, L. Zou, X. Cao, M. H. Engelhard, W. Liu, S. D. Burton, H. Lee, C. Niu, B. E. Matthews, Z. Zhu, C. Wang, B. W. Arey, J. Xiao, J. Liu, J.-G. Zhang, W. Xu, *Joule* **2019**, 3, 1662.
- [53] H. Lu, Y. Yuan, Z. Hou, Y. Lai, K. Zhang, Y. Liu, *RSC Adv.* **2016**, 6, 18186.
- [54] X. Ren, S. Chen, H. Lee, D. Mei, M. H. Engelhard, S. D. Burton, W. Zhao, J. Zheng, Q. Li, M. S. Ding, M. Schroeder, J. Alvarado, K. Xu, Y. S. Meng, J. Liu, J.-G. Zhang, W. Xu, *Chem* **2018**, 4, 1877.
- [55] X. Dong, Y. Lin, P. Li, Y. Ma, J. Huang, D. Bin, Y. Wang, Y. Qi, Y. Xia, *Angew. Chem., Int. Ed.* **2019**, 131, 5679.
- [56] X. Liu, A. Mariani, T. Diemant, M. E. D. Pietro, X. Dong, M. Kuenzel, A. Mele, S. Passerini, *Adv. Energy Mater.* **2022**, 12, 2200862.
- [57] J. Holoubek, M. Yu, S. Yu, M. Li, Z. Wu, D. Xia, P. Bhaladhare, M. S. Gonzalez, T. A. Pascal, P. Liu, Z. Chen, *ACS Energy Lett.* **2020**, 5, 1438.
- [58] Z. Yu, P. E. Rudnicki, Z. Zhang, Z. Huang, H. Celik, S. T. Oyakhire, Y. Chen, X. Kong, S. C. Kim, X. Xiao, H. Wang, Y. Zheng, G. A. Kamat, M. S. Kim, S. F. Bent, J. Qin, Y. Cui, Z. Bao, *Nat. Energy* **2022**, 7, 94.
- [59] X. Chen, X.-Q. Zhang, H.-R. Li, Q. Zhang, *Batteries Supercaps* **2019**, 2, 128.
- [60] M. J. Frisch, G. W. Trucks, H. B. Schlegel, G. E. Scuseria, M. A. Robb, J. R. Cheeseman, G. Scalmani, V. Barone, G. A. Petersson, H. Nakatsuji, X. Li, M. Caricato, A. V. Marenich, J. Blolino, B. G. Janesko, R. Gomperts, B. Mennucci, H. P. Hratchian, J. V. Ortiz, A. F. Izmaylov, J. L. Sonnenberg, D. Williams-Young, F. Ding, F. Lipparini, F. Egidi, J. Goings, B. Peng, A. Petrone, T. Henderson, D. Ranasinghe, et. al., *Gaussian 16, revision C.01*, Gaussian, Inc., Wallingford, CT, **2016**.
- [61] X. Liu, X. Shen, H. Li, P. Li, L. Luo, H. Fan, X. Feng, W. Chen, X. Ai, H. Yang, Y. Cao, *Adv. Energy Mater.* **2021**, 11, 2003905.
- [62] L. Xing, W. Li, M. Xu, T. Li, L. Zhou, *J. Power Sources* **2011**, 196, 7044.
- [63] T. Lu, F. Chen, *J. Comput. Chem.* **2012**, 33, 580.